Structural and dynamical properties of aqueous mixtures of pectin and chitosan

ARTICLE *in* EUROPEAN POLYMER JOURNAL · APRIL 2005

Impact Factor: 3.01 · DOI: 10.1016/j.eurpolymj.2005.02.028

5 AUTHORS, INCLUDING:

Marianne Hiorth
University of Oslo
27 PUBLICATIONS **447** CITATIONS
SEE PROFILE

Anna-Lena Kjøniksen
Østfold University College
122 PUBLICATIONS **2,334** CITATIONS
SEE PROFILE

Kenneth D Knudsen
Institute for Energy Technology
116 PUBLICATIONS **1,281** CITATIONS
SEE PROFILE

Available online at www.sciencedirect.com
SCIENCE DIRECT®
European Polymer Journal 41 (2005) 1718–1728
EUROPEAN POLYMER JOURNAL
www.elsevier.com/locate/europolj

Structural and dynamical properties of aqueous mixtures of pectin and chitosan

Marianne Hiorth [a,*], Anna-Lena Kjøniksen [b], Kenneth D. Knudsen [c], Sverre Arne Sande [a], Bo Nyström [b]

[a] Department of Pharmaceutics, School of Pharmacy, University of Oslo, P.O. Box 1068, Blindern, N-0316 Oslo, Norway
[b] Department of Chemistry, University of Oslo, P.O. Box 1033, Blindern, N-0315 Oslo, Norway
[c] Department of Physics, Institute for Energy Technology, P.O. Box 40, N-2027 Kjeller, Norway

Received 25 January 2005; accepted 25 February 2005
Available online 8 April 2005

Abstract

In this study phase separation, structure, and dynamics of aqueous pectin–chitosan mixtures of different ratios and a pure aqueous pectin sample have been investigated under various conditions by turbidimetry, SANS and dynamic light scattering (DLS). Only the mixture with $r = 0.75$ gelled upon decreasing the temperature (($r \equiv m_{\text{pectin}}/(m_{\text{pectin}} + m_{\text{chitosan}})$, where m denotes the mass of the considered component). The pure pectin sample ($r = 1$) did not gel and the decrease in temperature seemed to promote phase separation. The addition of chitosan reduced the tendency of pectin to phase separate in the mixtures of pectin and chitosan. The general trend when cooling the samples was that the turbidity and the growth of the turbidity became more pronounced as the amount of pectin in the mixture was increased. The wavelength dependence of the turbidity indicated a change of the conformation of pectin chains from an extended form to a more compact structure in pectin solutions without chitosan as the temperature decreased. This was not observed for the mixture of pectin and chitosan. SANS measurements revealed excess scattered intensity in the low wave vector area with the strongest upturn for the pure pectin sample ($r = 1$). DLS experiments showed longer slow relaxation times after a temperature quench for all samples, with the most pronounced effect for the mixture of pectin and chitosan with $r = 0.75$. The synergism between pectin and chitosan at high pectin contents ($r = 0.75$) generated large association complexes over time.

Keywords: Pectin; Chitosan; Turbidity; Dynamic light scattering; SANS

1. Introduction

When aqueous systems of different biopolymers are mixed together, the behavior of the individual polymer is usually affected and a synergism between the polymers emerges [1–6]. The interaction between unlike chains can be either more favorable or less favorable than interactions between like chains of each type. Mixed biopolymers are used in a wide range of applications [6–10], because of their ability to interact synergistically and provide material with controlled properties.

A semidilute aqueous mixture of pectin and chitosan with pH = 1.7 have been shown to gel upon cooling and

* Corresponding author. Tel.: +47 22 85 65 98; fax: +47 22 85 44 02.
E-mail address: marianne.hiorth@farmasi.uio.no (M. Hiorth).

0014-3057/$ - see front matter © 2005 Elsevier Ltd. All rights reserved.
doi:10.1016/j.eurpolymj.2005.02.028

the gelling temperature will be dependent of the mixture ratio of the polymers [11]. The gelation temperature is increased with an increasing amount of pectin until the ratio between pectin and chitosan (r) is 0.75. At low or very high values of r no temperature-induced gelation is observed. Evidence [12–17] is provided for a kinship between gelation and phase separation in the process of temperature-induced gelation of pectin and chitosan mixtures.

The gelling ability of pectin and chitosan in an acidic environment may be valuable for restricting drug release in the stomach as the gel layer may provide a protective barrier preventing drug release.

Pectins are anionic polysaccharides extracted from cell walls of most plants, consisting of a backbone of polygalacturonic acid. Pectins are usually classified according to the degree of methoxylation (DM): low methoxylated (LM) pectin with a DM < 50 and high methoxylated (HM) pectin DM > 50 [18]. The ability of pectins to form gels depend upon their DM grade. HM pectin may form a gel in the presence of for example sugar (cosolute) [19] and it has been reported that gelation can be induced through hydrogen bonds and hydrophobic interactions [20,21]. LM pectin is known to form gels in the presence of divalent ions [22,23]. When pectin and calcium interacts a gel network is formed with the well known egg-box structure [24]. Pectin has also been reported to interact with polymers of opposite charge, e.g., chitosan [11,25–27].

In the field of pharmaceutics, pectin and calcium have been investigated in many different formulations intended for colon drug delivery. This combination has been reported in the literature both for matrix tablets [28,29] and gel beads [30,31]. The combination of pectin and chitosan has also been investigated as a possible colonic drug delivery system most promising as a film coating [32–35].

Chitosan is a linear cationic polysaccharide prepared from chitin, found in shells of shrimps, lobsters and crabs consisting of a backbone of glucosamine. Chitosan is classified according to the degree of acetylation (or deacetylation; Dda) [36]. Chitosan may be valuable in controlled drug delivery for example as enteric-coated chitosan capsules to enhance uptake of insulin [37] and as microparticle for delivery of clozapin [38].

When pectin and chitosan are mixed in the pH range 3–6 a polyelectrolyte complex (PEC) is formed [39]. At this pH both polymers are charged. At low pH values (below pH = 2) pectin will be protonated and the importance of electrostatic interactions are suppressed, and an interaction between pectin and chitosan will probably take place via hydrogen bonding [11].

In this investigation we will evaluate the physical features of the macromolecular complexes formed in aqueous mixtures of pectin and chitosan. In addition we will compare the results from the mixtures with a pure aqueous pectin sample of the same concentration. Turbidity, small-angle neutron scattering (SANS) as well as dynamic light scattering (DLS) measurements have been carried out for this purpose. The aim of this work is to gain insight into phase separation, morphology, and dynamics of pectin–chitosan mixtures under various conditions. This knowledge is essential in the development of pharmaceutical formulations.

2. Experimental section

2.1. Materials and solution preparation

A low-methoxyl (LM) pectin citrus sample Pectin Classic CU701 (lot. no. 0903185) was obtained from Herbstreith & Fox GmbH, Germany. According to the specifications from the manufacturer, this sample has a DM of 35% and the galacturonic acid content is 88%. The raw materials were centrifuged for 12 h at 3800 rpm and dialyzed (Mw cut off 8000) against deionized water for seven days and freeze dried prior to use. The molecular weight was determined from capillary viscometry on dilute solutions of pectin dissolved in 1 wt% sodium hexametaphosphate pH = 4.5 (suppressing the tendency of forming aggregates) at 20 °C with the following Mark–Houwink equation $[\eta] = 9.55 \times 10^{-2} M^{0.73}$ (ml/g) [40]. The molecular weight was estimated to be 5×10^4 [11].

The chitosan sample (Seacure CL 313; batch no. 301-492-01) was prepared by Pronova Biopolymers (Drammen, Norway). According to the manufacturer the degree of deacetylation was 84%. From capillary viscometry at acid conditions (0.2 M sodium acetate/0.3 M acetic acid), the molecular weight was determined to be 2.2×10^5 [11] from intrinsic viscosity data $[\eta] = 7.6 \times 10^{-2} M^{0.76}$ (ml/g) [41]. This chitosan sample is water soluble only at acid pH and due to the presence of protonated amino groups it exhibits a polyelectrolyte character at low pH.

All samples were individually prepared by mixing (at 70 °C) aqueous stock solutions of the respective polymers in 0.1 M HCl at different mixture ratios r, defined as $r \equiv m_{\text{pectin}}/(m_{\text{pectin}} + m_{\text{chitosan}})$, where m denotes the mass of the considered component. Magnetic stirring at elevated temperatures (70 °C) for 1 h carefully mixed the samples. Most of the mixtures were prepared at a constant total polymer concentration of 1 wt% (semidilute samples), but some dilute mixtures were also prepared with a total polymer concentration of 0.1 wt%. Investigated mixtures were $r = 0.25$, $r = 0.5$ and $r = 0.75$. A pure pectin sample solved in 0.1 M HCl, $r = 1$ was also tested. A pH of approximately 1.7 was obtained for the mixtures in 0.1 M HCl. The pure pectin sample had a pH of approximately 1.

2.2. Turbidimetry

The transmittance of the different mixtures of pectin and chitosan was measured with a temperature controlled Helios Gamma (Thermo Spectronic, Cambridge, UK) spectrophotometer at different wavelengths according to the type of experiments. The apparatus is equipped with a temperature unit (Peltier plate) that gives a good temperature control over an extended time. The turbidity τ of the samples can be determined from the following relationship: $\tau = (-1/L)\ln(I_t/I_0)$ where L is the light path length in the cell (0.2 cm), I_t is the transmitted light intensity, and I_0 is the incident light intensity. The wavelength dependency of the turbidity may be related to the conformation of the polymer chains in the sample [42]. For particles much larger than the wavelength, the turbidity will be proportional to $\lambda^{-4+\gamma}$. The value of γ is one for rods and two for spheres and coils [43].

The temperature scan measurements were carried out at 400 nm by cooling the samples (0.5 °C/min) from 90 to 20 °C. The samples were heated up again from 20 to 90 °C at the same rate as the cooling rate. The cloud points (CP) of the samples were determined from the temperature scan measurements, and was taken as the time of the initial steep increase in the turbidity. The quenching experiments were performed by a rapid decrease in temperature from 90 to 55 °C or from 90 to 20 °C (400 nm). The wavelength scan experiments (400–800 nm) were carried out at 55 and 20 °C. The solvent was 0.1 M HCl.

2.3. Dynamic light scattering

Dynamic light scattering experiments were carried out with the aid of a standard laboratory-built light scattering spectrometer with vertically polarized incident light of wavelength $\lambda = 514.5$ nm supplied by an argon ion laser (Lexel laser, model 95). The beam was focused onto the sample cell through a temperature-controlled chamber (temperature controlled to within ±0.05 °C) filled with refractive index matching silicone oil. The sample solutions were filtered at high temperature (90 °C) through 5.0 μm filters (Millipore) directly into precleaned 10 mm NMR tubes (Wilmad Glass Company) of highest quality. The dynamics of the scattering process can be explored on a length scale of q^{-1}, where q is the wave vector magnitude defined as $q = 4\pi n \sin(\theta/2)/\lambda$. Here λ is the wavelength of the incident light in a vacuum, θ is the scattering angle, and n is the refractive index of the solution. The full homodyne intensity autocorrelation function $g^2(q,t)$ was measured for different pectin and chitosan mixtures at a scattering angle of 90°. The temperature was quenched from 90 °C to 20 °C and the first measurement was done 1 min after quenching. Correlation functions were then measured at different times after quenching. The correlation functions were recorded in the real time "multiple-τ" mode of the correlator, in which 256 time channels were logarithmically spaced over an interval ranging from 0.2 μs to almost 1 h. The results presented in this work will deal with dilute polymer concentrations (0.1%) and temperatures (quench from 90 to 20 °C) where the systems can be considered as ergodic. In this case, the scattered field obeys Gaussian statistics and the measured correlation function $g^2(q,t)$ can be related to the theoretically amenable first-order electric field correlation function $g^1(q,t)$ by the Siegert relationship [44].

$$g^2(q,t) = 1 + B \mid g^1(q,t)\mid^2 \tag{1}$$

where B is usually treated as an empirical factor.

In the case of associating polymer systems, one usually observes [45–50] a bimodal time autocorrelation function consisting of one single-exponential decay followed at longer times by a stretched exponential.

$$g^1(t) = A_f \exp(-t/\tau_f) + A_s \exp[-(t/\tau_{se})^{\beta}] \tag{2}$$

with $A_f + A_s = 1$. This relationship is found to capture the characteristic features of the present systems. The parameters A_f and A_s are the amplitudes for the fast and slow relaxation modes, respectively. When time correlation functions from DLS at long wavelengths in the semidilute regime are analyzed, the first term (short-time behavior) on the right-hand side of Eq. (2) yields the mutual diffusion coefficient $D_m(\tau_f^{-1} = D_m q^2)$, which reflects a concerted motion of polymer chains relative to the solvent. The second term (long-time behavior) is expected to be associated with disengagement relaxation of individual chains [51,52] or cluster relaxation [53]. The variable τ_{se} is some effective slow relaxation time, and the stretched exponent β ($0 < \beta \leq 1$) is an indication of the width of the distribution of relaxation times. The β variable has been interpreted [51] as a measure of inhomogeneity or disorder effects of the system, and the specific value of β depends on the topological dimension of the modeled cluster. The mean slow relaxation time is given by

$$\tau_s \equiv \int_0^{\infty} \exp[-(t/\tau_{se})^{\beta}]\,dt = (\tau_{se}/\beta)\Gamma(1/\beta) \tag{3}$$

where $\Gamma(\beta^{-1})$ is the gamma function of β^{-1}.

In the analysis of the correlation function data, a non-linear fitting algorithm (a modified Levenberg–Marquardt method) was utilized to obtain best-fit values of the parameters A_f, τ_f, τ_{se}, and β appearing on the right-hand side of Eq. (2). A fit was considered satisfactory if there were no systematic deviations in the plot of the residuals of the fitted curve.

The total concentration of polymer was 0.1 wt% for all samples. The solvent was 0.1 M HCl.

2.4. Small-angle neutron scattering (SANS)

Small-angle neutron scattering experiments were carried out at 23 °C at the SANS installation at the IFE

reactor at Kjeller, Norway. The instrument is equipped with a liquid hydrogen moderator, which shifts the D_2O moderated thermal neutron spectrum (intensity maximum at approximately 1 Å) toward longer wavelengths. The wavelength was set with the aid of a velocity selector (Dornier), using a high FWHM for the transmitted beam with a wavelength resolution ($\Delta\lambda/\lambda$) of 20% and maximized flux on the sample. The beam divergence was set by an input collimator (18.4 or 12.2 mm diameter) located 2.2 m from the sample, together with a sample collimator that was fixed to 4.9 mm. The solutions were filled in 2 mm quartz cuvettes. To avoid evaporation of the solvent the cuvettes were sealed with a teflon cap. The measuring cells were placed onto a copper-base for good thermal contact and mounted in the sample chamber. The chamber was evacuated to reduce air scattering. The detector was a 128×128 pixels, 59 cm active diameter, ^{3}He-filled RISØ type detector, which is mounted on rails inside an evacuated detector chamber. In SANS measurements one usually prefers D_2O to H_2O as a solvent due to lower background and often also better contrast. However here, H_2O was used as solvent since D_2O destroys the gelling ability of the samples. Each complete scattering curve is composed of three independent series of measurement, using three different wavelength-distance combinations (5.1 Å/1.0 m, 5.1 Å/3.4 m, and 10.2 Å/3.4 m). These combinations were utilized to yield scattering vectors q in the range of 0.008–0.25 $Å^{-1}$. Standard reductions of the scattering data, including transmission corrections, were conducted by incorporating data collected from the empty cell, the beam without the cell, and the blocked-beam background. When relevant, the data were transformed to an absolute scale (coherent differential cross-section $(d\Sigma/d\Omega \sim I(q))$ by calculating the normalized scattered intensity from direct beam measurements [54]. The total concentration of polymer was 1 wt% for all samples. The solvent was 0.1 M HCl.

3. Results and discussion

Before the results are presented it may be instructive to give some information about the different pectin and chitosan mixtures. A semidilute mixture of pectin and chitosan solved in 0.1 M HCl will normally gel when the temperature is decreased. The gelling temperature and the ability to gel is dependent of the composition between pectin and chitosan [11]. A pure 1 wt% pectin sample will not gel in this pH range, but if the pectin concentration is increased a white gel will be formed. By decreasing the pH between 1.6 and 3 and increase the concentration a true gel will be formed [55,56]. In this study only the mixture where $r = 0.75$ gelled upon decreasing the temperature and an incipient gel was formed at 40 °C.

In 0.1 M HCl the pectin chains are almost uncharged while the chitosan chains are positively charged so no polyelectrolyte complex will be formed. To form a gel, network connectivity must be established. The tendency for pectin to associate through hydrogen bonding when decreasing the temperature is believed to be important to establish connectivity [11].

3.1. Turbidimetry

Fig. 1 shows the temperature dependences of the turbidity for three different pectin and chitosan mixtures, $r = 0.25$, $r = 0.5$ and $r = 0.75$ all solved in 0.1 M HCl as well as a pure pectin sample $r = 1$ in 0.1 M HCl when the temperature is decreased from 90 to 20 °C and then increased from 20 to 90 °C. The turbidity of the $r = 0.25$ mixture is low and practically constant during the cooling and heating process, whereas for $r = 0.5$, $r = 0.75$ and $r = 1$ there is an abrupt increase in the turbidity when the sample is cooled down below approximately 60 °C. A pure chitosan sample ($r = 0$) was clear at all temperatures.

The general trend when cooling the samples is that the turbidity and the growth of the turbidity become more pronounced as the amount of pectin in the mixture is increased (see the inset plot that shows the turbidity at 20 °C). An increase in the turbidity is an indication of poorer thermodynamic conditions leading to large-scale heterogeneities and the formation of lumps of associated polymer. When the temperature is decreased, the

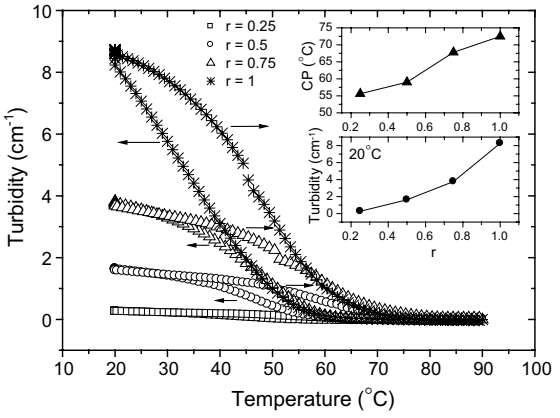

Fig. 1. Temperature dependence of turbidity, characterized by measurements of absorbance (400 nm) during cooling ← and heating → for different mixtures of pectin and chitosan ($r = 0.25$, 0.5 and 0.75) and a pure pectin sample ($r = 1$). Total polymer concentration is 1 wt%. The upper inset plot shows the cloud point for the different samples, whereas the lower inset plot shows the turbidity at 20 °C for the different samples.

thermodynamic conditions become worse and pectin starts to aggregate. For the pure pectin sample $r = 1$, cooling leads to a macroscopic phase separation. For the $r = 0.75$ mixture, the thermodynamic conditions are also deteriorated upon cooling the sample but the addition of chitosan suppress the tendency of pectin to phase separate. This may be a result of a small increase of the pH (increased charge density) when chitosan is added and improved thermodynamics. The interaction between pectin and chitosan inhibits the pectin chains to self-associate.

Pectin chains can take both a twofold structure and a threefold structure [57]. At pH values where most of the carboxyl groups are ionized (around 3.5) the chain will be stiffened and extended by intramolecular electrostatic repulsion, giving local conformation close to the extended twofold structure. Reduction in charge density by lowering pH will allow the chain to adopt a more compact arrangement close to the threefold structure [55]. At the pH values presented in this study, around 1 for the pure pectin sample and 1.7 for the mixtures of pectin and chitosan, the conformation of pectin is assumed to be threefolded and rather compact. Threefolded chains can possible associate into larger assemblies. The threefolded structure can be disrupted by heating the sample [55].

When the samples are heated form 20 to 90 °C the thermodynamic conditions are improved and the turbidity decreases (Fig. 1). If the turbidity at low temperatures is connected to hydrogen bonded chains lumped together, it seems reasonable that the turbidity decreases when the temperature is increased because hydrogen bonds are disrupted at elevated temperature.

However, melting occurs at a higher temperature than gel formation/phase separation upon cooling. The samples become totally clear only when the temperature is raised to 90 °C again. This may be related to slow kinetics of structure formation on cooling and enhancement of thermal stability by aggregation, respectively. It is evident from the heating and cooling curves in Fig. 1 that the hysteresis effect decreases and disappears at $r = 0.25$ where the amount of chitosan in the mixture is high. This is in good agreement with studies performed on LM pectin in HCl at pH = 1.6 [55].

For the pectin–chitosan systems of different composition, the cloud point temperatures have been estimated from the cooling cycle to the point where the first deviation of the turbidity from the baseline occurred. At high temperatures the systems are homogeneous, but when the temperature is lowered below a critical value (CP) of the mixture, a macroscopic phase separation evolves. It is evident that the cloud point temperature rises strongly as the contents of pectin in the mixture increases (see the lower inset plot of Fig. 1). This clearly demonstrates that CP declines as the amount of chitosan in the mixture increases.

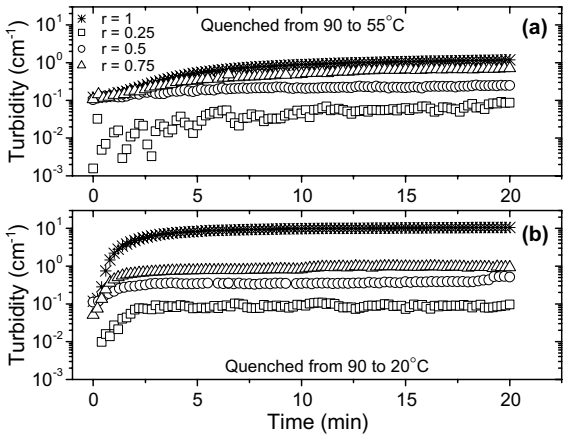

Fig. 2. Turbidity measurements when the sample is quenched from (a) 90 to 55 °C and from (b) 90 to 20 °C for different mixtures of pectin and chitosan ($r = 0.25$, 0.5 and 0.75) and a pure pectin sample ($r = 1$). Total polymer concentration is 1 wt%.

The effects of temperature quenching on the turbidity are depicted for different pectin–chitosan ratios in Fig. 2. At 70 °C, the turbidity of all the samples is almost zero. When the temperature is quenched from 90 to 55 °C, the change in the turbidity is small, especially for the samples with $r = 0.25$ and $r = 0.5$. For the pure pectin sample with $r = 1$ and the $r = 0.75$ mixture the rise in the turbidity is palpable and the growth of aggregates starts soon after the quench. When the temperature is quenched from 90 to 20 °C a more drastic change occurs for the samples; the turbidity commences to increase almost immediately after the temperature quench for all samples, and after a short time (≈5 min) the curves level out. The change in turbidity is strongest for the pure pectin sample ($r = 1$), and it is less pronounced as the chitosan contents in the mixture increases. A temperature quench from 90 to 20 °C gives rise to a much steeper and marked rise for the $r = 0.75$ mixture than what is observed with a quenching depth from 90 °C to 55 °C (Fig. 3). Theoretical studies [12–17] have established the interference between gelation and macroscopic phase separation. The smoother rise of the turbidity (Fig. 3) with time at the higher quenching temperature (55 °C) probably reflects that the growth of the cross-linking zones is slower than at 20 °C. Even though the gelation temperature of this pectin/chitosan composition is lower (40 °C) than 55 °C it is clear that large-scale associations have evolved above the gel point, but these junctions zones are not sufficient to establish the connectivity necessary for the gel network.

Fig. 4 shows the time evolution of the turbidity upon a temperature quench from 90 to 20 °C for pectin solutions of different concentration and for a pectin–chitosan mixture ($r = 0.75$) at a total polymer concentration

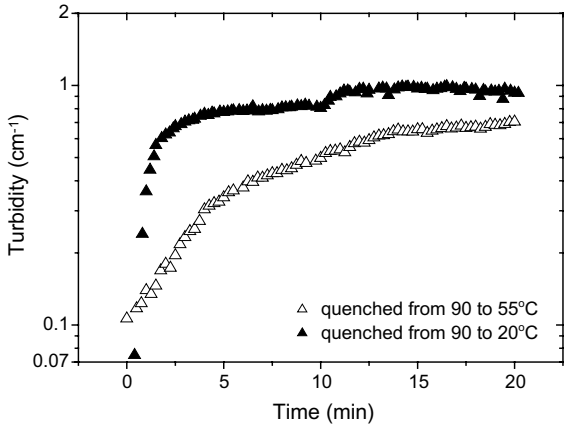

Fig. 3. Turbidity measurements for a mixture of pectin and chitosan ($r = 0.75$) quenched as indicated. Total polymer concentration is 1 wt%.

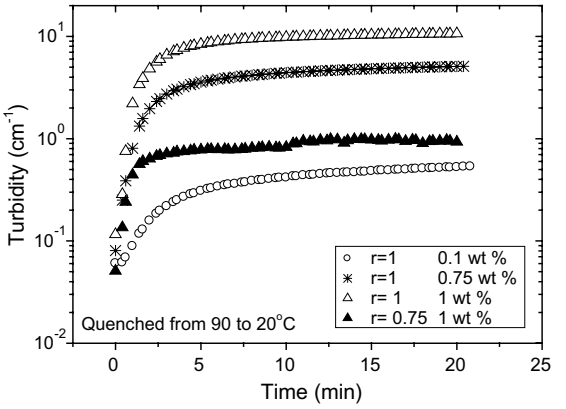

Fig. 4. Turbidity measurements of a mixture of pectin and chitosan ($r = 0.75$, total polymer concentration is 1 wt%) quenched from 90 to 20 °C and at different concentrations (0.1 wt%, 0.75 wt% and 1 wt%) of a pure pectin sample ($r = 1$).

of 1 wt%. The profile of the turbidity curves are the same, but for the pectin solutions the rise of the turbidity is more marked as the polymer concentration increases. This is expected because higher pectin concentration promotes the formation of larger aggregation complexes. Addition of chitosan leads to amended thermodynamic conditions and smaller aggregates are created. Furthermore, the repulsive electrostatic interactions in the pectin–chitosan complex prevent further macroscopic phase separation of pectin. As a consequence, the values of the turbidity are lower than for the corresponding pectin solution without chitosan.

Turbidity values of aqueous solutions of pure pectin ($r = 1$, both 1 wt% and 0.1 wt%) and mixtures of pectin and chitosan ($r = 0.75$ and $r = 0.5$) were used to evaluate the shape parameter γ ($\lambda^{-4+\gamma}$) (Fig. 5). The slopes

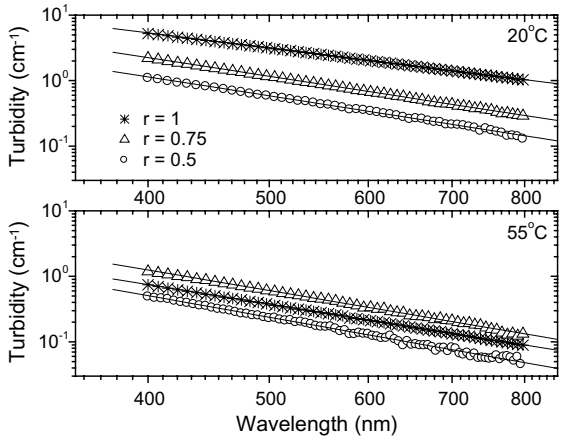

Fig. 5. Wavelength dependence (scan from 400–800 nm) of the turbidity for different pectin–chitosan ratios ($r = 0.5$ and $r = 0.75$) and a pure pectin sample ($r = 1$). Total polymer concentration is 1 wt%.

($n = \gamma - 4$) obtained from the linear plots of log τ versus log λ yielded the values of γ. This means that the value of n can be used to indicate the shape of particles which cause scattering. This type of procedure has been utilized previously [42] in the analysis of turbidity results.

For all pectin–chitosan compositions γ was below 1 when the temperature was 55 °C (Table 1). At this temperature the chains will probably have an extended random conformation. For the mixtures of pectin and chitosan the γ value increased to a certain degree when the temperature was decreased to 20 °C, but the conformation of the polymers is still believed to be extended. In sharp contrast is the pure pectin sample, where γ is changing from 1 to 1.63 for the 1 wt% sample and to 1.9 for the 0.1 wt% pectin sample. The change in the γ value indicates a conformational change from an extended form to a more compact form (coils or globules). This may indicate a collapse of the network in the pectin samples when the temperature is decreased.

3.2. SANS results

To gain insight into the structure, induced both by the gelation process and the phase separation of pectin, SANS experiments were carried out on three different samples with $r = 0.25$, $r = 0.75$ and $r = 1$ (the total polymer concentration is 1 wt%) all solved in 0.1 M HCl (Fig. 6). A conspicuous feature of Fig. 6 is the upturn of the scattered intensity $I(q)$ at low q values. This trend is most pronounced for the pure pectin sample $r = 1$, and it becomes weaker as the chitosan contents in the mixture increases. At $r = 0.25$ virtually no upturn of the scattered intensity is visible. In the low q regime the scattered intensity is governed by large-scale fluctuations of the polymer concentration and a strong upturn of the

Table 1
Slopes n and turbidity form factors γ for different pectin–chitosan ratios at different temperatures and concentrations

Composition	Concentration (%)	Temperature (°C)	n	γ	Interpretation
$r = 1$	1	55	−3.07	0.93	Transition from extended to compact form
		20	−2.37	1.63	
$r = 1$	0.1	55	–	–	Transition from extended to compact form
		20	−2.09	1.91	
$r = 0.75$	1	55	−3.25	0.75	Extended form
		20	−2.92	1.08	
$r = 0.5$	1	55	−3.38	0.61	Extended form
		20	−2.97	1.03	

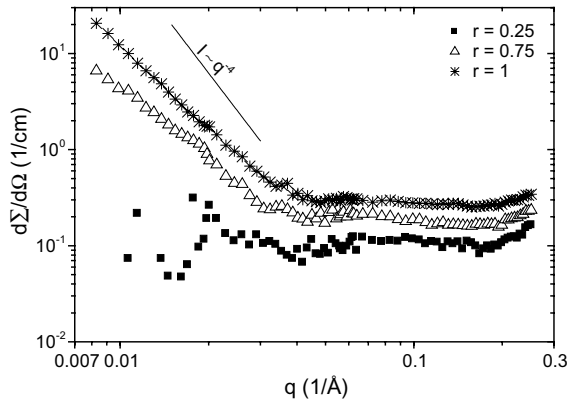

Fig. 6. A comparison of SANS data (on a log–log plot of scattered intensity $I(q)$ versus q) for different pectin–chitosan ratios ($r = 0.25$ and $r = 0.75$) and a pure pectin sample ($r = 1$).

intensity has been interpreted in terms of multichain domains [58] or large association structures. This behavior is compatible with turbidimetry results (cf. Fig. 1), where higher turbidity values are observed as the pectin contents of the sample increases.

After the contribution from the solvent H_2O to the signal has been subtracted a qualitative analysis can be performed. In the low q area ($q = 0.009$–0.015 Å^{-1}) the slope can be determined from a log–log plot of the intensity versus $q(I(q) \sim q^{-\alpha})$. The values of the power law exponent α for the samples with $r = 0.75$ and $r = 1$ are 2.2 and 2.8, respectively. It has been argued [59] that a high value of α reflects the presence of smooth interfaces and an exponent of 4 suggests a Porod scattering law [60]. The strong upturn in the scattering at low q in this study probably results from the presence of large size clusters or local inhomogeneities. A possible explanation

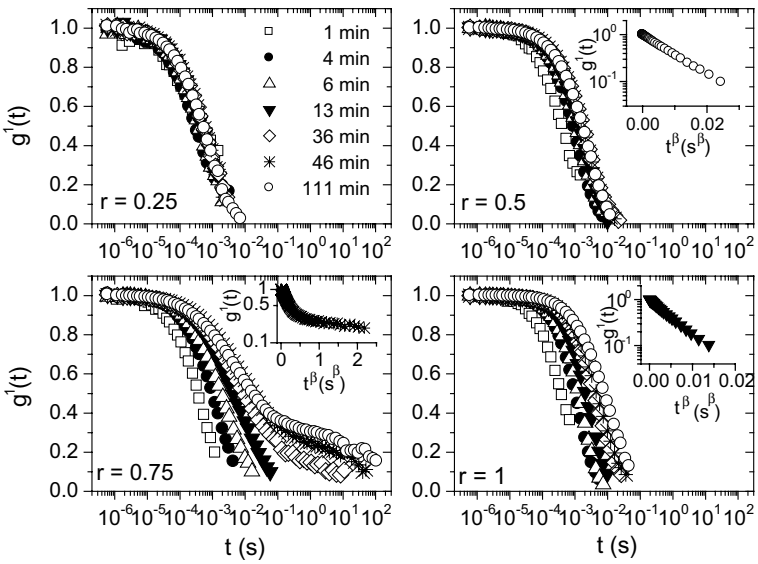

Fig. 7. First-order field correlation function versus time after quenching of different pectin–chitosan ratios ($r = 0.25$, 0.5 and 0.75) and a pure pectin sample ($r = 1$). Total polymer concentration is 0.1 wt%. The curves are fitted with the help of Eq. (2). The inset plots demonstrate the stretched exponential character of the correlation functions at long time.

of a power law exponent between 2 and 3 may be the presence of a diffuse interface between regions of different concentrations, due to incomplete phase separation. At high chitosan contents ($r = 0.25$), the tendency of macroscopic phase separation is suppressed and no large-scale structures are formed. The upturn in the scattering profile at low q values has been reported in several SANS studies [61–67] on polymers of various natures and values of α from approximately 2 to 4 have been found.

3.3. Dynamic light scattering

Dynamic light scattering (DLS) measurements have been carried out on samples with different pectin–chitosan compositions and with a total polymer concentration of 0.1 wt%. The reason for measuring on only dilute samples is that at higher polymer concentrations problems arise because of incipient phase separation and gelation. As a result, the analysis of the correlation functions is complicated by the emergence of multiple-scattering and non-ergodic features. These complications have been avoided in this work.

Normalized time correlation data of the aqueous pectin sample ($r = 1$) and the aqueous mixtures of pectin–chitosan with $r = 0.25$, $r = 0.5$ and $r = 0.75$ at various time after temperature quenching from 90 to 20 °C are depicted in Fig. 7 in the form of semilogarithmic plots. The inset in Fig. 7 shows semilogarithmic plots of $g^1(t)$ as a function of t^β for the compositions indicated. This type of plot yields straight lines for functions that can be represented by stretched exponentials. Within experimental error the long-time behaviors of the correlation functions are well described by straight lines. A comparison of the correlation functions reveals that there is a progressive slowing down of the relaxation process at longer times after quenching, both for the pectin–chitosan mixtures and the pure pectin sample. The shift of the slow relaxation mode toward longer times is apparent for the pure pectin sample ($r = 1$). In the case of the pectin–chitosan mixtures, it is obvious that the relaxation process is slowed down as the amount of pectin in the mixture increases. At $r = 0.75$, a long-time tail of the correlation function evolves in the course of time and this special feature for this composition signalizes strong interactions between pectin and chitosan chains. The long-time relaxation tails observed for the 0.75 mixture of pectin–chitosan suggest that association structures are formed, both when the temperature is decreased and also when the time after quenching is increased.

The time dependences of the fast (τ_f) and the slow (τ_s) relaxation time after quenching from 90 to 20 °C for the indicated samples are depicted in Fig. 8a and b. The fast and the slow relaxation times show similar time evolutions, but with higher values for τ_s. The fast mode is probably associated with the relaxation of single molecules and small aggregates, whereas the slow mode monitors the dynamics of large interchain structures. In the case of the pectin–chitosan mixtures, the time-induced rise of τ_f and τ_s become gradually more pronounced as the pectin contents of the mixture increases. This finding suggests that the rate of aggregate growth and the size of the aggregates increase more strongly at higher percentage of pectin. The synergism between pectin and chitosan at high pectin contents seems to give rise to large association complexes over time. In the evolution of these huge species, the conjecture is that hydrogen bonds play an important role. The fact that the values of the relaxation times at longer times are lower for the pure pectin solution ($r = 1$) than for the mixture with the highest pectin contents ($r = 0.75$) indicates that small amounts of chitosan in the sample promote the growth of multichain structures, and thereby slow the relaxation process of chain or cluster disengagement. Fig. 8c shows the turbidity evolution for a temperature quench from 90 to 20 °C for mixtures of pectin and chitosan ($r = 0.5$ and $r = 0.75$) and the pure pectin samples ($r = 1$) with a total polymer

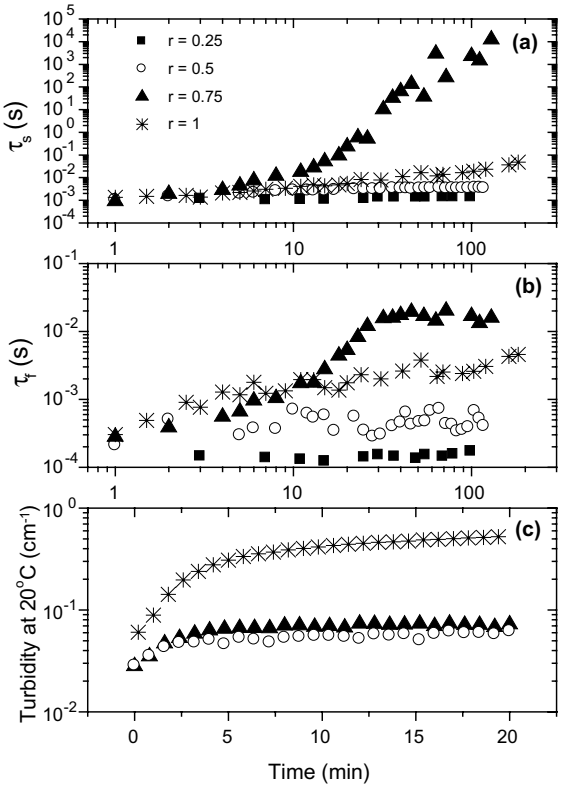

Fig. 8. (a) The fast relaxation times and (b) the slow relaxation times as a function of time after quenching and (c) the turbidity versus time after quenching of pectin–chitosan mixtures of the ratios indicated and a pure pectin sample. Total polymer concentration of the samples is 0.1 wt% and DLS was conducted at a scattering angle of 90°.

concentration of 0.1 wt%. The turbidities of the mixtures of pectin and chitosan exhibit a modest increase in the course of time, whereas a marked rise is observed for the pure pectin sample indicating phase separation of pectin.

4. Conclusions

In this work we have investigated the temperature dependence of the turbidity of pectin–chitosan mixtures of different compositions and compared the results with a pure pectin sample of the same polymer concentration. Upon cooling the samples to 20 °C a steep rise in the turbidity was observed for all samples, except the mixture of pectin and chitosan with $r = 0.25$. This effect was largest for the pure pectin sample ($r = 1$). When heating the samples the turbidity declines. The cooling and heating cycles of the pectin–chitosan mixtures with different ratios ($r = 0.5$, $r = 0.75$, and $r = 1$) revealed hysteresis effects. When the samples were quenched from 90 to 55 °C or from 90 to 20 °C the same trend was observed, with a steep rise in the turbidity for the pure pectin sample ($r = 1$). The rise in the turbidity of the pure pectin sample is probably connected to poor thermodynamics and the close proximity to phase separation. The thermodynamics in the mixtures of pectin and chitosan is probably improved, thereby leading to lower turbidity. The wavelength dependence of the turbidity indicated that the pectin chains in the pure pectin sample ($r = 1$, 1 wt%) were transformed from an extended conformation at 55 °C to a more compact structure at 20 °C. No such transformation of the morphology was found in the mixtures of pectin and chitosan.

The SANS results showed a distinct upturn of scattered intensity in the low q-area for the pure pectin sample ($r = 1$) and the mixture of pectin and chitosan ($r = 0.75$). This is probably related to the presence of large size clusters or local inhomogeneities.

The time correlation function data obtained form the DLS experiments on dilute solutions were analyzed by a model where the initial decay could be described by a single exponential followed by a stretched exponential at longer times. A comparison of the correlation functions disclosed a progressive slowing down of the relaxation process at longer times after quenching, both for the pectin–chitosan mixtures and the pure pectin sample. The appearance of the long-time tail of the relaxation process for the $r = 0.75$ mixture of pectin and chitosan signalizes strong interactions between pectin and chitosan chains. This effect is observed both when the temperature is decreased and also when the time after quenching is increased.

The picture that emerges form this study is that a semidilute mixture of pectin and chitosan ($r = 0.75$, 1 wt%) gels upon decreasing the temperature to 20 °C. Both time and temperature promotes the formation of association structures between pectin and chitosan. The presence of chitosan inhibits the phase separation of pectin. A pure aqueous pectin sample ($r = 1$, pH $\sim$ 1, 1 wt%) exhibits phase separation when the temperature is decreased form 90 to 20 °C and no connectivity of the network is established.

Acknowledgments

B.N., K.D.K., and S.A.S. gratefully acknowledge support from the Norwegian Research Council through a NANOMAT Project (158550/431). K.D.K. also thanks the Marie Curie Industry Host Project (Contract No. G5TR-CT-2002-00089) for support.

References

[1] Picout DR, Richardson RK, Rolin C, Abeysekera RM, Morris ER. Ca2+-induced gelation of low methoxy pectin in the presence of oxidised starch. Part 1. Collapse of network structure. Carbohydr Polym 2000;43(2):113–22.

[2] Picout DR, Richardson RK, Morris ER. Co-gelation of calcium pectinate with potato maltodextrin. Part 1. Network formation on cooling. Carbohydr Polym 2000;43(2):133–41.

[3] Gilsenan PM, Richardson RK, Morris ER. Associative and segregative interactions between gelatin and low-methoxy pectin. Part 3. Quantitative analysis of co-gel moduli. Food Hydrocolloids 2003;17(6):751–61.

[4] Morris ER. Polysaccharide synergism—more questions than answers? In: Harding SE, Hill SE, Mitchell JR, editors. Biopolymer mixtures. Nottingham: Nottingham University Press; 1995. p. 247–88.

[5] Bergfeldt K, Piculell L, Linse P. Segregation and association in mixed polymer solutions from Flory–Huggins model calculations. J Phys Chem 1996;100(9):3680–7.

[6] Iliopoulos MB, Audebert R. In: Dubin P, Bock J, Davis R, Schulz DN, Thies C, editors. Macromolecular complexes in chemistry and biology. Berlin: Springer; 1994.

[7] Wakerly Z, Fell JT, Attwood D, Parkins D. Studies on drug release from pectin/ethylcellulose film-coated tablets: A potential colonic delivery system. Int J Pharm 1997;153(2):219–24.

[8] Macleod GS, Fell JT, Collett JH, Sharma HL, Smith AM. Selective drug delivery to the colon using pectin:chitosan:hydroxypropyl methylcellulose film coated tablets. Int J Pharm 1999;187(2):251–7.

[9] Li S, Wang X, Zhang X, Yang R, Zhang H, Zhu L, et al. Studies on alginate-chitosan microcapsules and renal arterial embolization in rabbits. J Control Release 2002;84(3):87–98.

[10] Huguet ML, Dellacherie E. Calcium alginate beads coated with chitosan: Effect of the structure of encapsulated materials on their release. Process Biochem 1996;31(8):745–51.

[11] Nordby MH, Kjøniksen A-L, Nyström B, Roots J. Thermoreversible gelation of aqueous mixtures of pectin and chitosan. Rheology. Biomacromolecules 2003;4(2): 337–43.
[12] Tanaka F. Phase formation of associating polymers: Gelation, phase separation and microphase formation. Adv Colloid Interf Sci 1996;63:23–40.
[13] Tanaka F, Ishida M. Elastically effective chains in transient gels with multiple junctions. Macromolecules 1996;29(23): 7571–80.
[14] Liu Y, Pandey RB. Sol–gel phase transitions in thermoreversible gels: Onset of gelation and melting. J Chem Phys 1996;105(2):825–36.
[15] Ishida M, Tanaka F. Theoretical study of the postgel regime in thermoreversible gelation. Macromolecules 1997; 30(13):3900–9.
[16] Semenov AN, Rubinstein M. Thermoreversible gelation in solutions of associative polymers. 1. Statics. Macromolecules 1998;31(4):1373–85.
[17] Tanaka F, Stockmayer WH. Thermoreversible gelation with junctions of variable multiplicity. Macromolecules 1994;27(14):3943–54.
[18] Thakur BR, Singh RK, Handa AK. Chemistry and uses of pectin—a review. Crit Rev Food Sci Nutr 1997;37(1): 47–73.
[19] Bulone D, Martorana V, Xiao C, San Biagio PL. Role of sucrose in pectin gelation: Static and dynamic light scattering experiments. Macromolecules 2002;35(21): 8147–51.
[20] Rolin C. Pectin. In: Whistler RL, BeMiller JN, editors. Industrial gums: Polysaccharides and their derivatives. San Diego: Academic Press; 1993.
[21] Oakenfull DG. The chemistry of high-methoxyl pectins. Chem Technol Pectin 1991:87–108.
[22] Morris VJ. Functional properties of food macromolecules. London: Elsevier Applied Science Publisher; 1986.
[23] Rees DA. Structure, conformation, and mechanism in the formation of polysaccharide gels and networks. Adv Carbohydr Chem Biochem 1969;24:267–332.
[24] Grant GT, Morris ER, Rees DA, Smith PJC, Thom D. Biological interactions between polysaccharides and divalent cations: The egg-box model. FEBS Lett 1973;32(1): 195–8.
[25] Marudova M, MacDougall AJ, Ring SG. Pectin–chitosan interactions and gel formation. Carbohydr Res 2004; 339(11):1933–9.
[26] Meshali MM, Gabr KE. Effect of interpolymer complex-formation of chitosan with pectin or acacia on the release behavior of chlorpromazine HCl. Int J Pharm 1993;89(3): 177–81.
[27] Yao KD, Liu J, Cheng GX, Lu XD, Tu HL, DaSilva JAL. Swelling behavior of pectin/chitosan complex films. J Appl Polym Sci 1996;60(2):279–83.
[28] Sungthongjeen S, Pitaksuteepong T, Somsiri A, Sriamornsak P. Studies on pectins as potential hydrogel matrices for controlled-release drug delivery. Drug Dev Ind Pharm 1999;25(12):1271–6.
[29] Ahrabi SF, Madsen G, Dyrstad K, Sande SA, Graffner C. Development of pectin matrix tablets for colonic delivery of model drug ropivacaine. Eur J Pharm Sci 2000;10(1): 43–52.
[30] Munjeri O, Collett JH, Fell JT. Amidated pectin hydrogel beads for colonic drug delivery—An in vitro study. Drug Delivery 1997;4(3):207–11.
[31] Sriamornsak P, Nunthanid J. Calcium pectinate gel beads for controlled release drug delivery: I. Preparation and in vitro release studies. Int J Pharm 1998;160(2):207–12.
[32] Macleod GS, Collett JH, Fell JT. The potential use of mixed films of pectin, chitosan and HPMC for bimodal drug release. J Control Release 1999;58(3):303–10.
[33] Hiorth M, Tho I, Sande SA. The formation and permeability of drugs across free pectin and chitosan films prepared by a spraying method. Eur J Pharm Biopharm 2003;56(2):175–82.
[34] Hiorth M, Versland T, Heikkila J, Tho I, Sande SA. Immersion coating of pellets with calcium pectinate and chitosan, submitted for publication.
[35] Sriamornsak P, Puttipipatkhachorn S. Chitosan–pectin composite gel spheres: Effect of some formulation variables on drug release. Macromol Symp 2004;216:17–21.
[36] Roberts GAF. Chitin chemistry. Houndsmille: Macmillan; 1992.
[37] Tozaki H, Komoike J, Tada C, Maruyama T, Terabe A, Suzuki T, et al. Chitosan capsules for colon-specific drug delivery: Improvement of insulin absorption from the rat colon. J Pharm Sci 1997;86(9):1016–21.
[38] Agnihotri SA, Aminabhavi TM. Controlled release of clozapine through chitosan microparticles prepared by a novel method*1. J Control Release 2004;96(2):245–59.
[39] Yao KD, Tu HL, Cheng F, Zhang JW, Liu J. pH-sensitivity of the swelling of a chitosan–pectin polyelectrolyte complex. Angew Makromol Chem 1997;245:63–72.
[40] Anger H, Berth G. Gel-permeation chromatography and the Mark–Houwink relation for pectins with different degrees of esterification. Carbohydr Polym 1986;6(3): 193–202.
[41] Rinaudo M, Milas M, Ledung P. Characterization of chitosan—influence of ionic-strength and degree of acetylation on chain expansion. Int J Biol Macromol 1993; 15(5):281–5.
[42] Erbil C, Sezai Sarac A. Description of the turbidity measurements near the phase transition temperature of poly(*N*-isopropyl acrylamide) copolymers: The effect of pH, concentration, hydrophilic and hydrophobic content on the turbidity. Eur Polym J 2002;38(7):1305–10.
[43] Oster G. IIIA Optical, spectroscopic, and radioactivity methods. In: Weissberger A, Rossiter BW, editors. Physical methods of chemistry. New York: Wiley; 1977.
[44] Siegert AJF. Massachusetts Institute of Technology, 1943.
[45] Nyström B, Walderhaug H, Hansen FK. Dynamic crossover effects observed in solutions of a hydrophobically associating water-soluble polymer. J Phys Chem 1993; 97(29):7743–52.
[46] Nyström B, Lindman B. Dynamic and viscoelastic properties during the thermal gelation process of a nonionic cellulose ether dissolved in water—in the presence of ionic surfactants. Macromolecules 1995;28(4):967–74.
[47] Narayanan J, Deotare VW, Bandyopadhyay R, Sood AK. Gelation of aqueous pectin solutions: A dynamic light scattering study. J Colloid Interf Sci 2002;245(2):267–73.
[48] Kjøniksen A-L, Iversen C, Nyström B, Nakken T, Palmgren O. Light scattering study of semi-dilute aqueous

systems of chitosan and hydrophobically modified chitosans. Macromolecules 1998;31(23):8142–8.
[49] Tsianou M, Kjøniksen AL, Thuresson K, Nyström B. Light scattering and viscoelasticity in aqueous mixtures of oppositely charged and hydrophobically modified polyelectrolytes. Macromeolcules 1999;32(9): 2974–82.
[50] Kjøniksen A-L, Hiorth M, Nyström B. Temperature-induced association and gelation of aqueous solutions of pectin. A dynamic light scattering study. Eur Polym J 2004;40(11):2427–35.
[51] Douglas JF, Hubbard JB. Semiempirical theory of relaxation: Concentrated polymer solution dynamics. Macromolecules 1991;24(11):3163–77.
[52] Wang CH, Zhang XQ. Quasielastic light scattering and viscoelasticity of polystyrene in diethyl phthalate. Macromolecules 1993;26(4):707–14.
[53] Ngai KL. Dynamics of semidilute solutions of polymers and associating polymers. Adv Colloid Interf Sci 1996;64: 1–43.
[54] Wignall GD, Bates FS. Absolute calibration of small-angle neutron scattering data. J Appl Crystallogr 1987;20(1): 28–40.
[55] Gilsenan PM, Richardson RK, Morris ER. Thermally reversible acid-induced gelation of low-methoxy pectin. Carbohydr Polym 2000;41(4):339–49.
[56] Lootens D, Capel F, Durand D, Nicolai T, Boulenguer P, Langendorff V. Influence of pH, Ca concentration, temperature and amidation on the gelation of low methoxyl pectin. Food Hydrocolloids 2003;17(3):237–44.
[57] Cesaro A, Ciana A, Delben F, Manzini G, Paoletti S. Physicochemical properties of pectic acid. I. Thermodynamic evidence of a pH-induced conformational transition in aqueous solution. Biopolymers 1982;21(2): 431–49.
[58] Ermi BD, Amis EJ. Influence of backbone solvation on small angle neutron scattering from polyelectrolyte solutions. Macromolecules 1997;30(22):6937–42.
[59] Horkay F, Hecht A-M, Grillo I, Basser PJ, Geissler E. Experimental evidence for two thermodynamic length scales in neutralized polyacrylate gels. J Chem Phys 2002; 117(20):9103–6.
[60] Glatter O, Kratky O. Small angle X-ray scattering. London: Academic Press; 1982.
[61] Lal J, Bastide J, Bansil R, Boue F. Behavior of free linear chains of polystyrene in a network of methyl methacrylate in toluene. Macromolecules 1993;26(22):6092–9.
[62] Bastide J, Candau SJ. Structure of gels as investigated by means of static scattering techniques. In: Cohen Addad JP, editor. Physical properties of polymeric gels. Chichester: Wiley; 1996. p. 143–295.
[63] Rouf-George C, Munch J-P, Schosseler F, Pouchelon A, Beinert G, Boue F, et al. Thermal and quenched fluctuations of polymer concentration in poly(dimethylsiloxane) gels. Macromolecules 1997;30(26):8344–59.
[64] Hecht A-M, Horkay F, Geissler E. Neutron scattering investigations on a bimodal polymer gel. J Phys Chem B 2001;105(24):5637–42.
[65] Knudsen KD, Lauten RA, Kjøniksen A-L, Nyström B. Rheological and structural properties of aqueous solutions of a hydrophobically modified polyelectrolyte and its unmodified analogue. Eur Polym J 2004;40(4):721–33.
[66] Bu H, Kjøniksen A-L, Knudsen KD, Nyström B. Rheological and structural properties of aqueous alginate during gelation via the Ugi multicomponent condensation reaction. Biomacromolecules 2004;5(4):1470–9.
[67] Thorgeirsdottir TO, Kjøniksen A-L, Knudsen KD, Kristmundsdottir T, Nyström B. Viscoelastic and structural properties of pharmaceutical hydrogels containing monocaprin. Eur J Pharm Biopharm 2005;59(2):333–42.